Chapter 5

Amino Acids in Aqueous Solution

5.1 The Effect of pH on Lysine in Solution

5.1.1 Introduction

In the previous chapter, the focus was mainly on the behavior of ions in solution. The effect of concentration, solvent, as well as pH have been investigated; furthermore, alkali metal ions as well as transition metal ions have been studied. In this chapter, the investigation will be extended from ions to molecules, more specifically toward the behavior of amino acids in solution. Amino acids are the building blocks of proteins, and hence protein structure and reactivity are dependent on the specific properties of the incorporated amino acids. Particularly relevant for the understanding of biological activity, though, is the effect of water on the structure, both geometric and electronic, of amino acids. Especially the amino acids side chains have a strong influence on how the protein behaves in water. Water, in fact, takes part in a wide range of reactions within the cell, and it is, at various amounts, an integral part of all proteins. Moreover, the particular structure of the solvated amino acid is very sensitive to the pH of the solution; this is one reason why pH regulation is important in living organisms [111].

In the study presented in this chapter, x-ray photoelectron (XPS) spectroscopy [11, 112, 113], has been used to identify the electronic structural signature of individual nitrogen and carbon atoms in the amino acid lysine in liquid water environment. The XPS technique has been introduced in chapter

2.1, and the experimental setup has been discussed in chapter 3. Biological activity is influenced by the pH of the water as it determines whether or not certain functional group are charged, and hence it drives structural modifications. In this study we thus focus on the changes of the XPS spectra as a function of pH. In acid aqueous solution amino acids exist as cations, where the amino group is protonated. At intermediate pH amino acids form charge-neutral (dipolar) zwitterions, where the amino group is protonated, but the carboxylic group is not. In basic solution amino acids exist as anions, with an unprotonated neutral amino group. For lysine, the butylamine side chain is responsible for its basic reaction in aqueous solution. Fig.5.1 shows the structure of the lysine molecule for the different charge states. Below pH 9 both amino groups are protonated (I). Near the isoelectric point, around pH 9, the α-amino group is protonated and the amino group of the side chain is not (II). Above pH 10.5 both amino groups are deprotonated (III). This study will show that these changes of the functional groups lead to considerable and well-resolved energy shifts (so-called chemical shifts) of the N1s core-level electron binding energies (BE). It is even possible to experimentally resolve chemical shifts of the C1s core levels of carbon atoms in the immediate vicinity of the amino moiety. This highlights the local sensitivity of core-level photoemission to even through-bond interaction. In this study, the experimental energy shifts are found to be in good qualitative agreement with the DFT calculations. Furthermore, it is not only possible to assign specific spectral contributions to a specific nitrogen or carbon atom site in the lysine molecule, the data can also indicate whether or not solvent water molecules are H-bonded through the hydrogens at the amino groups.

Although structural properties of amino acids have long been an area of intense research, surprisingly few electron spectroscopic studies were devoted to the actual liquid water-amino acid interactions, which are so crucial in biological systems. In fact, the cationic and anionic forms are unique to the liquid phase. Gas-phase amino acids, on the other hand, exclusively exist in the neutral (molecular) form and in the condensed case amino acids are present in the zwitterionic form. This considerably complicates the comparison between gas and solid phase spectroscopic data, since condensation and charge-state contributions are not easily distinguishable.

NEXAFS and photoelectron spectroscopy (PES), are probably among the most versatile techniques for studying the local electronic structure. The standard amino acids have been extensively investigated by NEXAFS [114–119], XPS [120–127] and electron energy-loss spectroscopy [118]. Due to the technical

difficulties, the investigations were carried out either on thin solid films or in the gas phase. Most noteworthy are two recent NEXAFS studies at the nitrogen K-edge of aqueous amino acids [4, 5]. The authors were able to resolve changes in the pre-edge spectrum, which enabled them to conclude whether or not the hydrogens of the ammonium moiety participate in forming H bonds with the solvating water molecules.

PES studies from aqueous solutions are in general scarce, and no data were yet reported for amino acids in aqueous solution. These studies have only recently become possible after overcoming problems with the detection of electrons above the vaporizing water surface, and with the complexity of generating a stable free liquid water surface in high vacuum (as described in Section 3.4). PES provides complimentary information to XAS, probing occupied rather than empty states. Furthermore, with PES absolute binding energies, even of solvated species, are accessible. The major advantages are the variable probing depth sensitivity (as a function of the electron kinetic energy of the photoelectrons), and the possibility to address the carbon 1s level, which in absorption is often complicated by strong absorption by the optical components of the beamline itselves.
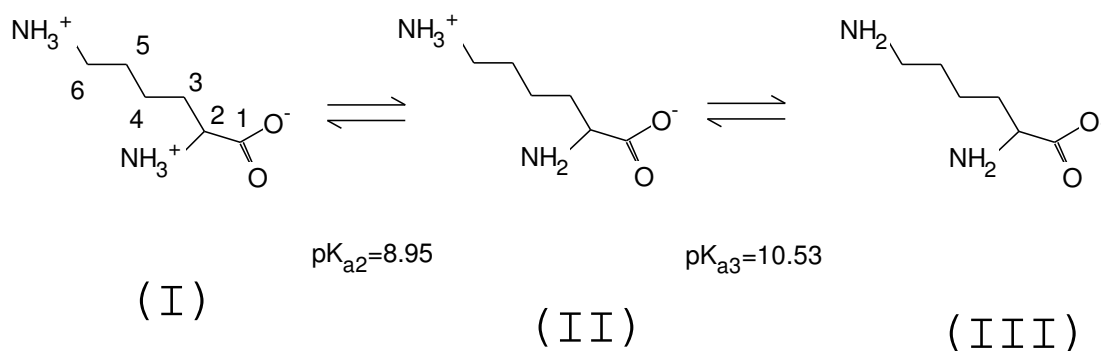

Figure 5.1: Lewis structure of the amino acid lysine at different pH values. Depending on the pH value two (I), one (II) or none (III) of the amino groups are protonated. The carbon atoms of the molecule are numbered from 1 - 6, starting from the carboxyl carbon number 1.

In this section, the applicability of x-ray photoelectron spectroscopy to obtain charge and site specific electronic structural information of biomolecules in aqueous solution is demonstrated. Changing the pH of an aqueous solution of lysine from acidic to basic reveals nitrogen 1s and carbon 1s chemical shifts

to lower binding energies. As we will see, these shifts are associated with the sequential protonation of the two amino groups, which affects both charge state and hydrogen bonding to the water solvation shell. The N1s chemical shift, 2.2 eV, is considerably larger than the various C1s shifts, as the carbon atoms sense the charge changes at a larger distance, through the aliphatic side chain. The assignments agree with the calculated energies of lysine$_{(aq)}$ for different pH using Tomasi's polarized continuum model. Details about the theoretical model are found in section 2.2.1.

5.1.2   Results and Discussion

The XPS setup as has been described in section3.4 has been used. The energy resolution of the U41 PGM beamline was about 200 and 450 meV at 600 and 1200 eV photon energy, respectively. The resolution of the hemispherical energy analyzer was constant with kinetic energy (KE), about 200 meV, at the pass energy of 20 eV. A typical count rate at a photon energy of 600 eV was 10^3 per second. The calibration of the electron kinetic energies was with respect to the O1s binding energy of liquid water, which can be measured simultaneously with the C1s and N1s spectra.

S(+)-lysine monohydrochloride (for synthesis) was purchased from Merck, and was used without further purification. A $\cong$ 0.5 molar solution of lysine monohydrochlorode in highly demineralized water was used for all experiments. The pH value of the room-temperature solution was adjusted either with sulphuric acid or sodium hydroxide, the pH was controlled with a pH meter (766, Knick) equipped with a single-rod measuring cell (SE 100, Knick).

Nitrogen 1s

Nitrogen 1s XPS spectra of 0.5 M aqueous lysine solution, at pH 13.0, 9.5, and 5.5, were measured at a photon energy of 480 eV. The results are shown in Fig.5.2 a-c. Here the energy axis refers to electron binding energies (BE), and intensities are normalized to the photon flux. The absolute energy scale was fixed relative to the O1s bending energy (BE) of liquid water (538.1 eV [9]).

At pH 13, which corresponds to cationic structure (I) in Fig.5.1, the spectrum exhibits a single peak (N1) at 404.3 eV BE. Occurrence of a single N 1s peak is
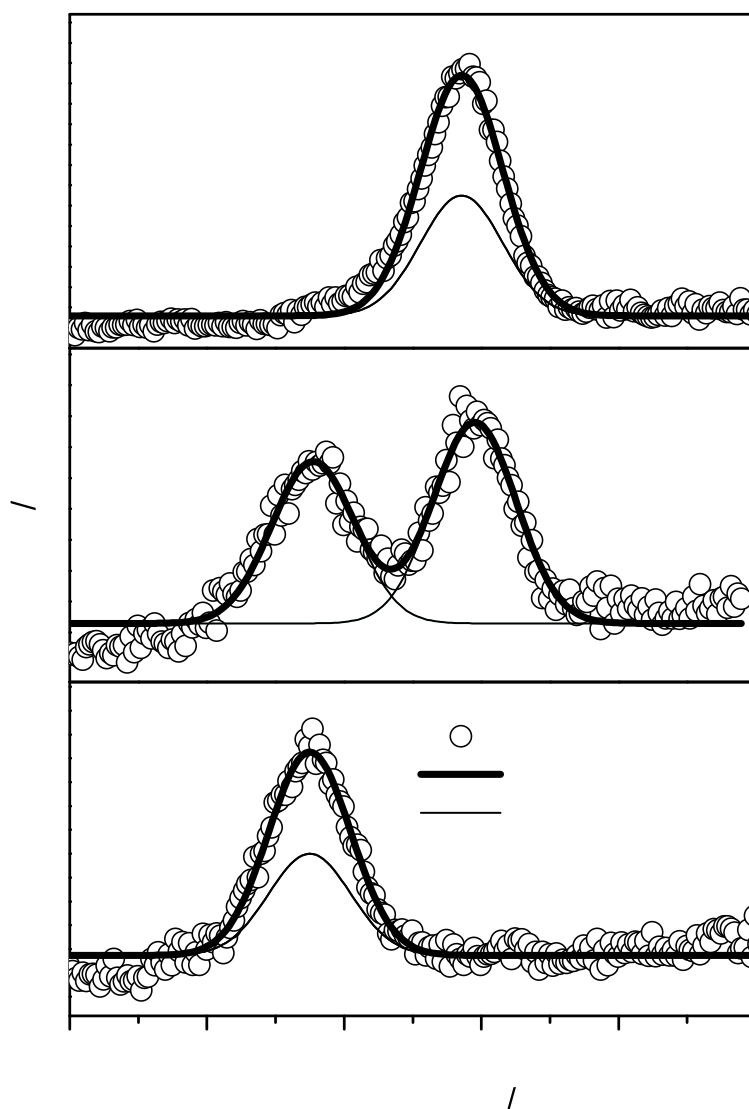
Figure 5.2: The N 1s binding energy depends on the pH value. a) At pH 13 both amino groups are neutral and have the same N 1s BE of 404.3 eV. b) Protonation of one amino groups increases its BE to 406.5 eV. As one amino group stays neutral the peak splits into two. c) At pH 5.5 both amino groups are protonated with the same BE of 406.5 eV for both nitrogen atoms.

consistent with both amino groups being neutral. At pH 9.5, i.e, for the case of one amino group being protonated and the other neutral (zwitterionic structure

(II)), N1 decreases in intensity and shifts to 404.1 eV, and a second peak (N2) appears at higher BE, 406.5 eV, having comparable signal intensity. Lowering of the pH to 5.5, at which point both amino groups are protonated (anionic structure (III)), results in the single peak N2, with the exact same peak position as found for pH 9.5, i.e 406.5 eV BE.

All XPS spectra were fitted with two gaussians, one for each nitrogen. Assuming similar cross sections and peak width for one measurement both gaussians were fitted with the same width but independent peak positions. For pH 13 (Fig.5.1a) and pH 9.5 (Fig.5.1b) the fitted full width at half maximum (FWHM) was 1.2 eV and for pH 5.5 (Fig.5.1b) 1.3 eV FWHM. For pH 13 and pH 5.5 both gaussians have exactly the same position, thus they can't be distinguished in Fig.5.1. This is consistent with the measured FWHM of N1 and N2 which are identical with the single gaussians.

In order to understand why at the lowest and highest pH studied just a single component, with no contribution from the other, is observed it is instructive to calculate the expected mole fraction of the different charge states as a function of pH. According to the law of mass action there is a distribution of the different charge states (I)-(III) depending on the pH value, as depicted in Fig. 5.3.

Yet, it can be seen that (with the actual pK_a values 10.53 and 8.95) for N^6 and N^2 (the nitrogen which is conected to carbon number 6, and carbond number 2 as shown in Fig.5.1), at pH 13 more than 99% of all lysine molecules exist in the anionic form (III), in agreement with the results in Fig.5.2a. Both amino groups are neutral, and the two nitrogens appear to have the same BE of 404.3 eV.

Lowering the pH value to 9.5, which is near the isoelectric point, causes the protonation of the nitrogen in the side chain and about 70% of all lysine molecules are present in the charge-neutral zwitterionic form (II). The remaining lysine molecules are in the charge states corresponding to (I) and (III), at equal amounts. The experimental ratio is much larger, though, which can be attributed to uncertainties in the determination of pH values ($\pm$ 0.3). Protonation (H^+) leads to a higher BE, which is due to columbic attraction between the photoelectron and the additional positive charge on the nitrogen atom. This explains the origin of a second peak in Fig.5.2b, at 2.2 eV larger BE. Finally, at pH 5.5 more than 99% of all lysine molecules exist with both nitrogens protonated (I), which yields a single peak in the spectrum of Fig.5.2c, at the same BE as the high-energy peak for (II). These spectral changes provide
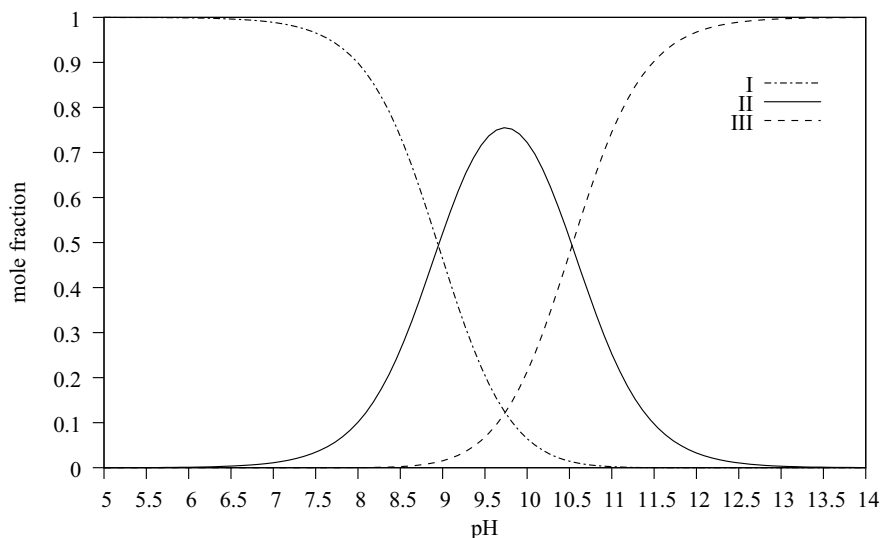
Figure 5.3: Mole fraction of three different charge states as a function of the pH value. The cationic (I) and the anionic (II) state can be populated to nearly 100%. However, the zwitterionic species (II) has a maximum of 75% at the isoelectric point (pH 9.74) due to the similar pK_a values of the two amino groups.

sufficient information to assign spectral features to the actual atomic site. Obviously peak N1 (404.3 eV BE) must be due to the neutral, and N2 (406.5 eV BE) arises from the protonated nitrogen.

The observed chemical shift of 2.2 eV is comparable to the one observed in solid state [120, 126, 127]. Notice that absolute N1s energies obtained in the film studies are with reference to the substrate Fermi energy, but a value of the Fermi energy was not given, which prevents a detailed comparison of liquid and film N1s energies. Nevertheless, the given BEs are similar to those measured in this experiment.

Within the resolution of this experiment the N 1s electron BE of both nitrogen atoms is the same for the neutral and protonated amino groups. The observed chemical shift agrees qualitatively with the calculations which give a BE of 402.9 eV for the neutral and 405.6 eV for the protonated amino groups. The calculated energies are in reasonably good agreement with the actual experimental values. Yet the calculated energy difference, 2.7 eV, is slightly larger than the experimental energy shift, 2.2 eV. This discrepancy is attributed to the considerable overestimation of the effect of the positive charge due to the

fact that H bonding is not explicitly included in the solvation model.

The results can be also rationalized in terms of the large dipole moment of water molecules and the amphoteric properties of water, which make water molecules strongly interact even with the neutral -NH$_2$ group. It is, in fact, not a priori clear if the neutral amino group acts as H bond donor or acceptor, or if this terminal group is completely solvated at all [4,5]. In order to give an answer one should discuss the various energies in greater detail. The N1s BE of aqueous lysine is 404.3 eV (neutral amino group), which is likely to be smaller than in the gas phase (here both nitrogens are neutral). To date, however, there is no experimental gas-phase value, but it is reasonable to assume that the value is close to the N 1s energy of glycine molecule, 405.58 eV [128], or n-butylamine, 404.85 eV [129].

The lower N1s energy in the liquid is a strong indication of increased electron density at the nitrogen site in aqueous environment, i.e. the amine nitrogen in aqueous lysine acts as H bond donor. Recent calculations show that anionic amino acids in small water clusters do not form hydrogen bonds with the water due to a strong interaction between the amino and carboxylic group [4,5]. Thus, intramolecular hydrogen bonds may be responsible for the observed shift in the liquid. However, it can't be ruled out that the limited cluster size was insufficient to describe bulk water at high pH as e.g. the possibility of OH$^-$ ions as H bond acceptor was not included in the calculations. Thus intra- or intermolecular hydrogen bonds with the amino group as donor may be responsible for the observed shift.

Switching from pH 13 to pH 9.5 causes protonation of the amino group of the side chain. This is clearly shown in Fig.5.2b. Surprisingly, this leads also to a 0.2 eV shift of the unprotonated α-amino group. The distance between the two amino groups is too large for a direct through-bond effect. Thus the shift is likely due to a rearrangement of the solvation shell or major changes of the present conformations. The zwitterionic structure allows e.g. a backfolding of the positively charged amino group to the negatively charged carboxylic group. Such intramolecular backfolding would be unlikely in case of the cationic species thus both nitrogens show the same BE in the protonated form.

C 1s binding energy

The C1s PE spectra of aqueous lysine are shown in Fig.5.4. All spectra were measured at the exact same pH as the N1s spectra in Fig.5.2; also the same photon energy was used, 480 eV. Comparative measurements at 380 eV, i.e., closer to the carbon K-edge gave the same results. Energies are presented as BE, as in Fig.5.2., and intensities are again normalized to the photon flux. The spectrum (circles are the experimental data) at pH 13 exhibits a smaller peak (C1) at 293.5 eV, and a larger and rather broad feature with maximum at 290.4 eV BE. The broad shape of the latter immediately suggests that this feature contains contributions from the various carbon atoms, in distinct local environment. At pH 9.5 a shoulder appears near 291.5 eV, while C1 remains entirely unaffected. The main change at pH 5.5 is the evolution of this shoulder into a distinct peak.

To analyze the structure of the measured C1s spectrum we fitted the spectrum with six equally shaped gaussians. Previous investigations on amino acids showed, that the C 1s of the carboxylic group has the highest binding energy [120, 123, 127]. Hence P1 at 293.4 eV is assigned to C^1. A total of six Gaussians, of identical width and intensity, were chosen as to represent the emission signal from each of the six carbon atoms in the lysine molecule. The (normalized) intensity of the (reference) Gaussian can be readily obtained from fitting C1. With this assignment of C1 one can also normalize the intensities of the three spectra of Figure 4 with respect to each other, since this peak stays well separated for all pH values. Then, the remaining part of the spectrum is reconstructed using five Gaussians with the exact same parameters, except for the energy. Photoionization cross section variations are small, and can be neglected.

For all three pH values the fits and the experimental spectra are in very good agreement, and peak positions of each Gaussian, in each spectrum, are highly unequivocal. The pH induced energy changes are hence accurate and quantitative, and it is possible to actually assign structural changes due to protonation at specific carbon site to a given Gaussian. The fitted and calculated binding energies are summarized in table 5.1.

Notice, though, that two Gaussians exactly overlap at the lowest binding energy. To infer the desired site-specific information, the most pronounced energy shifts, marked by the vertical lines, are considered in more detail.

peak Nr	assignment	pH 13		pH 9.5		pH 5.5	
		fitted	calculated	fitted	calculated	fitted	calculated
1	C1	293.4	279.2	293.4	279.2	293.4	280.1
2	C6	291.3	277.5	291.7	279.0	291.6	279.1
3	C2	290.8	277.4	291.0	277.5	291.3	278.9
4	C5	290.4	276.8	290.3	277.5	290.4	277.8
5	C3	289.9	276.8	290.0	276.9	289.9	277.6
6	C4	289.9	276.7	290.0	277.1	289.9	778.6

Table 5.1: Fitted and calculated BEs in eV. The peak numbers correspond to the gaussian numbers in Fig.5.4 and the assignment to the labels in Fig. 5.1.

To infer site-specific information we consider the most pronounced energy shifts, marked by the vertical lines in Fig.5.4, in more detail. G2 is shifted by 0.4 eV to a lower BE when going from pH 13 to 9.5 in Fig.5.4.b; this leads to the shoulder at 291.5 eV BE. Since protonation of the terminal amino group in the side chain is the main change at the former pH, G2 can be associated with the nearby carbon atom, C^6. Due to the considerable distance to the positive charge at the nitrogen site, the carbon 1s chemical shift is much smaller as compared to the nitrogen 1s energy shift (see Fig.5.2). G3 shows an initial smaller shift, 0.2 eV, and a 0.3 eV shift occurs between pH 9.5 and 5.5. In full analogy to the G2 case, we assign the latter G3 shift to the electron density change associated with the carbon atom C^2, as this is closest to the charged α-amino group. The former, smaller G3 energy shift is attributed to the fact, that close to the isoelectric point approximately 12% of the lysine molecules exist as cation 1 (Fig.5.3), which is not accounted for in our fit. Compared to the pH 13 case G3 is shifted by 0.5 eV, which is similar to the shift observed for G2.

The assignment of G4 is less clear as no distinct shift is observed. Obviously, the through-bond distance over which charge changes of the amino group can be sensed is not larger than the size of a methylen group. As C^6 has a slightly higher BE than C^2 (both directly connected to a nitrogen atom) a higher BE for C^5 would be expected than for C^3 (both separated by a methylen group from the nitrogen atom). We attribute the lower BE of C^2 to the +I effect of the deprotonated carboxylic group [130], which will effect C^3 more than C^5. Therefore, G4 is assigned to C^5, which also agrees with the calculations.

The two carbons, having the same BE (peaks G5 and G6), are assigned to

carbon atoms C^3 and C^4, respectively. The agreement between relative experimental and relative calculated energy changes, both summarized in Table 5.1, is fairly good. Although absolute theoretical energies are underestimated by approximately 5%, the relative BEs which are you used to assign spectral features to certain atoms are reliable. The assignment based on theory is the same as derived experimentally from the variation of the pH value (Table 5.1). All chemical shifts induced by the charge are overestimated in the calculations. We attribute this to the neglect of hydrogen bonds which are not included in the current method. This agrees with the larger discrepancies for nitrogen energies. The amino groups are expected to form strong hydrogen bonds with water, compared to the much weaker interaction of the aliphatic chain with the solvent. The shielding of the charge on the amino groups is not being properly described and as a result the theoretical shift is much larger than the experimental one. Therefore the through-bond interaction to the neighboring carbon atoms is also overestimated and the chemical shifts are too high. The through-bond interaction decreases with the distance to the localized charge and therefore the nitrogen is stronger affected than the carbon. As expected, and in agreement with previous studies, the C^1 carbon atom of the carboxyl group has the highest BE, whereas the carbons inside the aliphatic side chain (C^3 and C^4) have the lowest BE, and are not affected by the pH. The absolute BE for C^3 and C^4 is similar to the corresponding BE in n-hexane (290.09 eV), [131] i.e., they are not affected by the substituents. Furthermore, the calculations reveal the same order in BE obtained from the above qualitative discussion, and hence our calculations fully corroborate the assumption made in the spectral fit. Finally, the strong BE effect of carbon atoms adjacent to an amino group on charge states is in reasonably good agreement between experiment and theory. Yet, as we have already discussed for N1s, the C1s chemical shift is similarly overestimated in the solvation model used here.

5.1.3 Conclusion

Using the liquid microjet preparation technique for free liquid aqueous surfaces in vacuum in conjunction with XPS spectroscopy we have demonstrated that individual nitrogen and carbon atoms of aqueous lysine can be identified by their respective core-level binding energies. The technique is shown to to be sensitive to monitor charge densities modified by proton attachment Moreover, XPS measurements at different pH reveal a 2.2 eV nitrogen 1s chemical shift towards lower BEs, associated with the protonation of any of the amino groups of aqueous lysine. The sensitivity of photoemission is found to be high enough to distinguish

different carbon atoms of lysine in water. Here the C1s energies of carbon atoms next to the ammonium moiety are identified by a 0.5 – 0.3 eV chemical red-shift upon protonation. All experimental energies are found to be in good qualitative agreement with our tentative, moderate efforts, density functional theory calculations using commercially available software. These results highlight the potential of liquid photoemission to unravel electronic and structural details of biological molecules in their natural aqueous environment.
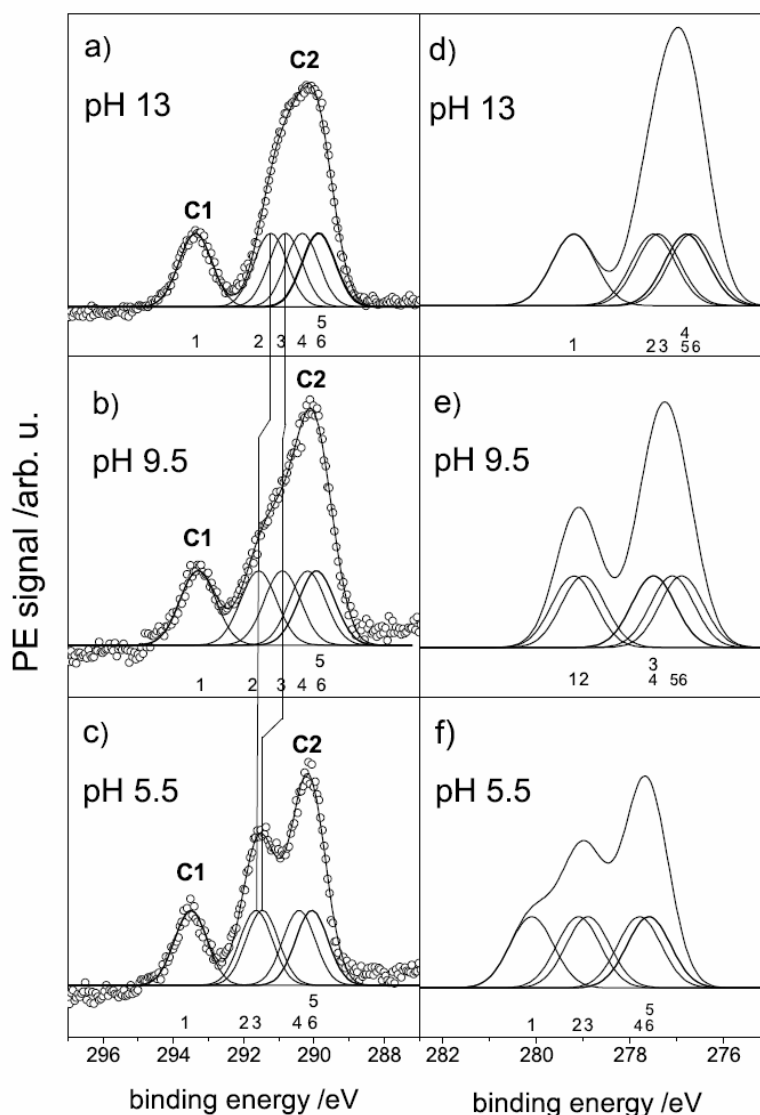
Figure 5.4: C1s XPS spectra of aqueous lysine, measured (a-c) and calculated (d-e). Sequential protonation of the amino groups causes a shift in the BEs of the respective adjacent carbon atoms (indicated by vertical lines). Intensities of the experimental spectra are normalized at the peak height of C1, which is the C1s emission from the carboxylic carbon atom, C1. Each experimental spectrum was fitted with six Gaussians (G1–G6) of identical widths and intensities. Small numbers are Gaussian peak labels, which should not be confused with the atom numbers in Fig.5.2. The simulated spectra were obtained by representing the emission from each carbon atom by a 1.1 eV wide Gaussian at the respective calculated BE.

5.2 Zn^{2+}-Amino Acid Complex Formation

5.2.1   Introduction

The complex formation between Zn^{2+} ions and histidine (His. see Fig.5.5.a) or cysteine (Cys. see Fig.5.5.b) is of biological interest, specifically for zinc finger proteins because His-Zn and Cys-Zn interactions are crucial for the function of this class of proteins. Zinc-binding proteins constitute approximately half of the transcription regulatory proteins in the human genome and are the most abundant class of proteins in the human proteome. The folding of the peptide chain around the Zn^{2+} ion takes place via Cys and His chelating the Zn^{2+} ion. This unit is an important part of the tertiary structure of the protein [132], as shown in Fig.5.6. Small changes in the local environment of Zn^{2+} can cause different protein folding and lead to different transcriptional regulation. For instance, numerous studies have shown that covalent bond modification of the nucleophilic zinc finger Cys-Thiolates can lead to inhibition of the human immunodeficiency virus (HIV) [133–135]. To determine the binding nature of this metallo-proteins at a fundamental level, it is helpful to understand the coordination and the structural effects of these amino acids on the central atom. These effects are identified either by investigating the metal center or by studying the ligand, namely, amino acids [136]. As has been shown before, the use of low molecular weight model compounds of these biological macromolecules is useful, and in some cases the only possible way to better understand the structure and function of their active sites [137].

Little is known about the electronic details of the His-Zn and Cys-Zn interaction, as many spectroscopic techniques have difficulties with the Zn^{2+} closed d-shell configuration [136,139,140]. On the other hand, the local structure for His and Cys chelating the zinc in the finger protein is very well known [138], where His chelates Zn^{2+} via the imidiazole ring, and Cys chelates Zn^{2+} via the SH group, as shown in Fig.5.6. In the protein, Cys can only chelate via the SH group since the NH_2 as well as COO^- group are forming the peptide bond. Similarly, His only has the imidiazole group available for chelation. Upon dissolving His or Cys as amino acids monomers in water, specifically at pH $\cong$ 5 (the natural pH of the solution upon dissolving $ZnCl_2$ with His or Cys), many several chelating groups are available. For instance, the His anion has three sites available for strong metal coordination, these are an imidazole nitrogen group
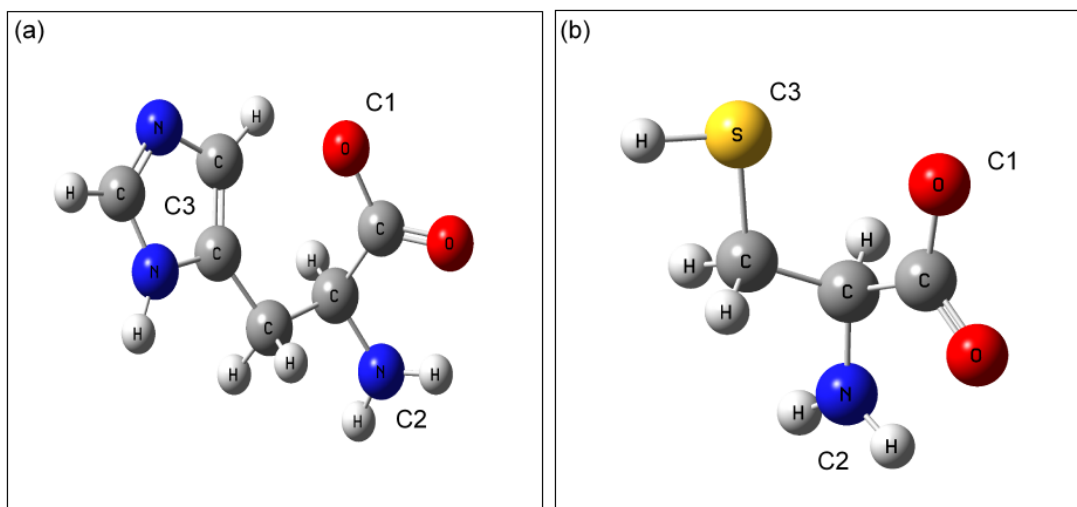
Figure 5.5: Chemical structure of (a) histidine anions, (b) cysteine anions. Each of them has three potentially chelating groups marked as C1, C2, and C3.
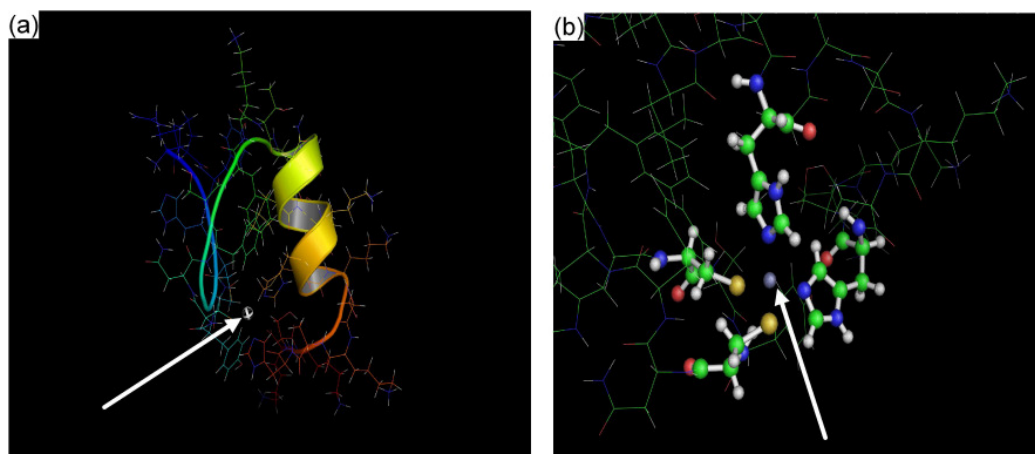

Figure 5.6: (a) The full structure of zinc finger from human enhancer binding-protein taken from the protein data base (3ZNF) [138]. (b) Local spherical visualization for the zinc atom and its coordination in 3ZNF (2 His, and 2 Cys). The arrow in both figures refers to the zinc atom in the center.

(C3), the COO^- group (C1) and amino-groups (C2) [141]. Stability constant measurements have shown that, if the metal ion is bonded through an imidiazole nitrogen and a carboxyl oxygen, while the amino nitrogen is protonated, a

complex $Zn(H - His)^{2+}$ is formed as shown in Fig.5.7.a. [139, 142, 143]. On the other hand, bonding through the amino-nitrogen and either an imidazole ring nitrogen or a carboxyl oxygen would give $Zn - His^+$, as shown in Fig.5.7.b. and 5.7.c. Neutron diffraction shows that histidine can act as a ter-dentate with cadmium [144] as is shown in Fig.5.7.d. However, NMR [145] and IR [146], as well as the potentiometric titration [147] support the protonated chelation in Fig.5.7.a. .
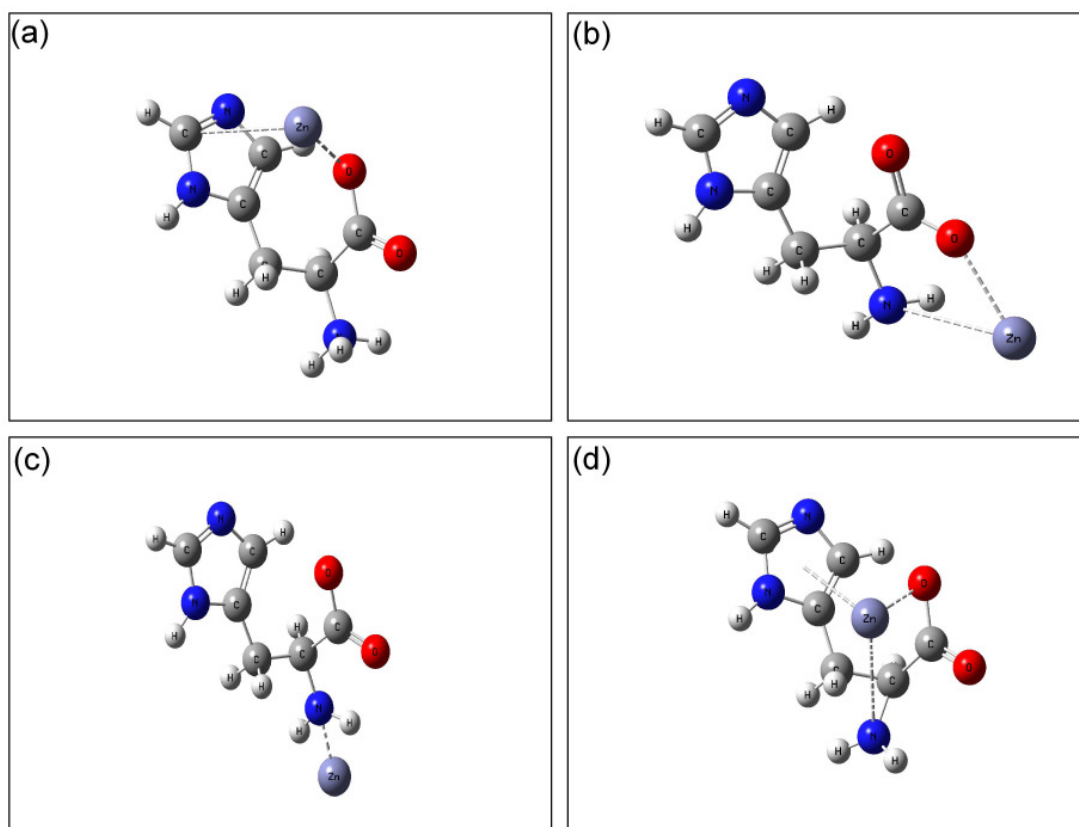

Figure 5.7: Reported chelation structures between Zn^{2+} and histidine.

The nature of complex formation between Zn^{2+} and Cys is discussed controversially in the literature. Perrin et. al. [148] using stability constant measurements have concluded, that $Zn - Cys^+$, and $ZnCys_2$ species are insignificant, while Arena et. al. [149] have shown the importance of these species in the solution. Another study has given details for the nature of complex formation between cysteine and Zn^{2+} [150], discussing the mono-dentate coordination of the carboxylate COO^-, thiolate (SH), as well as amino groups (NH_2) of

cysteine. Furthermore, studying the methyl ester form of the cysteine with Zn^{2+} [151] shows that the ability of forming $Zn - Cys_2$ species via the thiolate and the amino groups, increased upon rising the pH from 5 to 7, where at pH 7 100% of the complex is of the $ZnCys_2$ type complex. In general, one can summarize from the literature that cysteine can form a complex with Zn^{2+} ions via the carboxilic group with a protonated or non-protonated amino group as shown in Fig.5.8.a and Fig.5.8.b, or via the SH group as shown in Fig.5.8.c, or Fig.5.8.a bi-dentate complex via thiolate and amino group as shown in Fig.5.8.d.
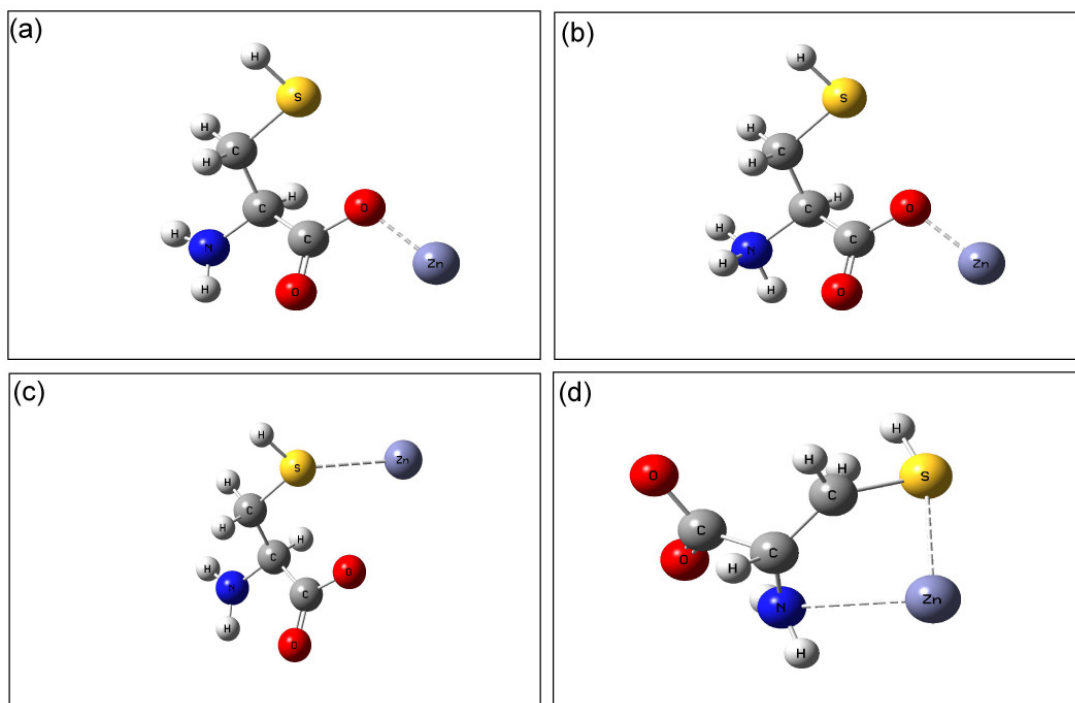

Figure 5.8: Reported chelation structures between Zn^{2+} and cysteine.

In this study, the nature of the interaction between the Zn^{2+} ions with His and Cys is investigated in aqueous solution at pH around 5. The experiments were carried out with the newly developed LIQUIDROM liquid spectroscopic end-station in soft x-ray regime at BESSYII [66,67]. This investigation will show that different chelation scenarios can be distinguished by the Zn^{2+} L-edge NEXAFS spectra in comparison to the spectra of reference complexes.

5.2.2   Results and Discussion

NEXAFS spectra for the L-edge of Zn^{2+} with histidine or cysteine in water are shown in Fig.5.9 and Fig.5.10, respectively. In both cases, the spectra are compared to NEXAFS from free Zn^{2+} ions in water. Note that the NEXAFS spectra in the cysteine experiment have a slightly different resolution than the spectra for histidine, since each series has been measured with slightly different monochromator parameters (which are kept constant within each series). In general the L-edge of the Zn^{2+} ions in the pure $ZnCl_2$ solution is characterized by two peaks, A, and B at energy 1018 eV, and 1021 eV respectively. According to the dipole selection rules [18], these peaks correspond to the transitions from $p_{3/2}$ states to s- and d-type states localized on the Zn^{2+}. Peak A is attributed to transitions from $p_{3/2}$ to empty s-states producing a relative sharp structure. Peak B can be then attributed to the transition from $p_{3/2}$ to the empty p-states, in accord with the unoccupied orbital energy ordering. Calculating the Zn^{+2} ion in water field using SCRF as discussed in section 2.2.1, confirm our speculation for the nature of the molecular orbitals which involve in the NEXAFS transition. Upon addition of amino acids to the 50 mM Zn^{2+} solution, a systematic variation for the NEXAFS spectra is observed as a function of increasing the amino acids concentration. This variation is qualitatively different for both amino acids. For His, peak A stays at the same energy, while peak B moves to lower absorption energy, as shown in Fig.5.9. For a concentration of 200 mM His, peak B has moved to 1019.3 eV. For Cys, upon increasing concentration, a shift of peak B to lower energies is observed, analogous to the His case. In contrast to His, a shift of peak A to higher absorption energy is observed for increasing Cys concentration as shown in Fig.5.10. For a concentration of 200 mM Cys, peak A has moved to 1018.8, and peak A has moved to 1020 eV absorption energy. For both His and Cys, a further increase of the amino acid / Zn^{2+} ratio in excess of $4 : 1$ did not change the spectra. Obviously, these changes in the local electronic structure at the Zn^{2+} ions are due to the formation of complexes between the Zn^{2+} ions and the amino acids.

At this point one can only speculate that the presence of the SH group in Cys - which is absent in His - is responsible for the different behavior of the two types of amino acids. A potential mechanism is a nucleophilic attack of the Cys by the SH group on the Zn^{2+} ions, possibly involving the COO^- group, while His can make the neuclophilic attack via the NH_2 group alone or together with COO^-. In the following we shed more light on the complex formation and its effect on the NEXAFS spectra by investigating several model systems.
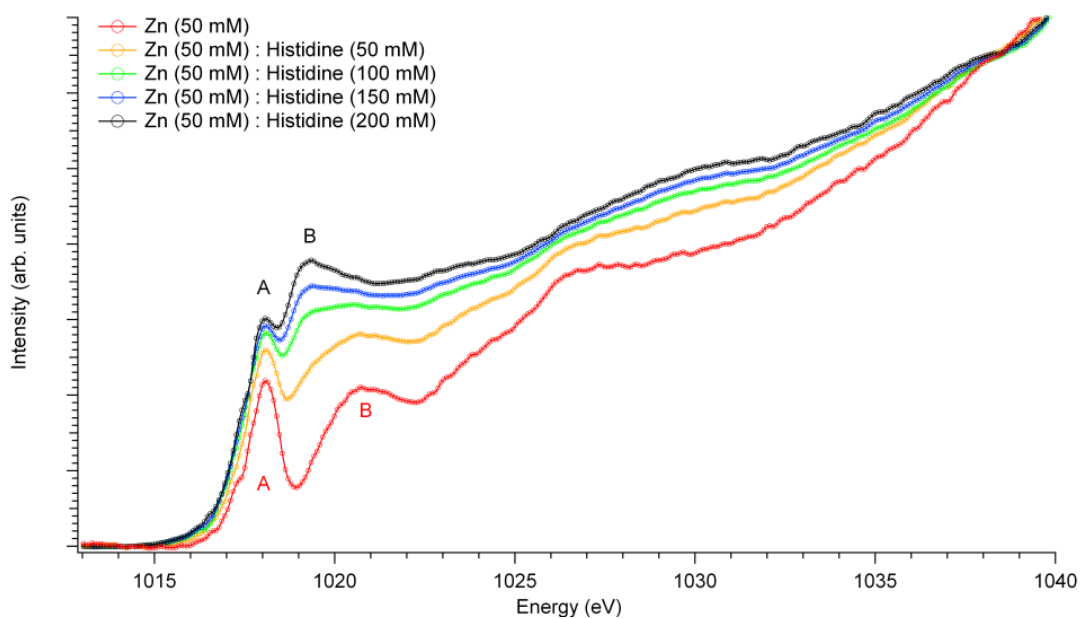
Figure 5.9: Zn^{2+} L-NEXAFS spectra for different concentration ratio of Zn:histidine at pH 5
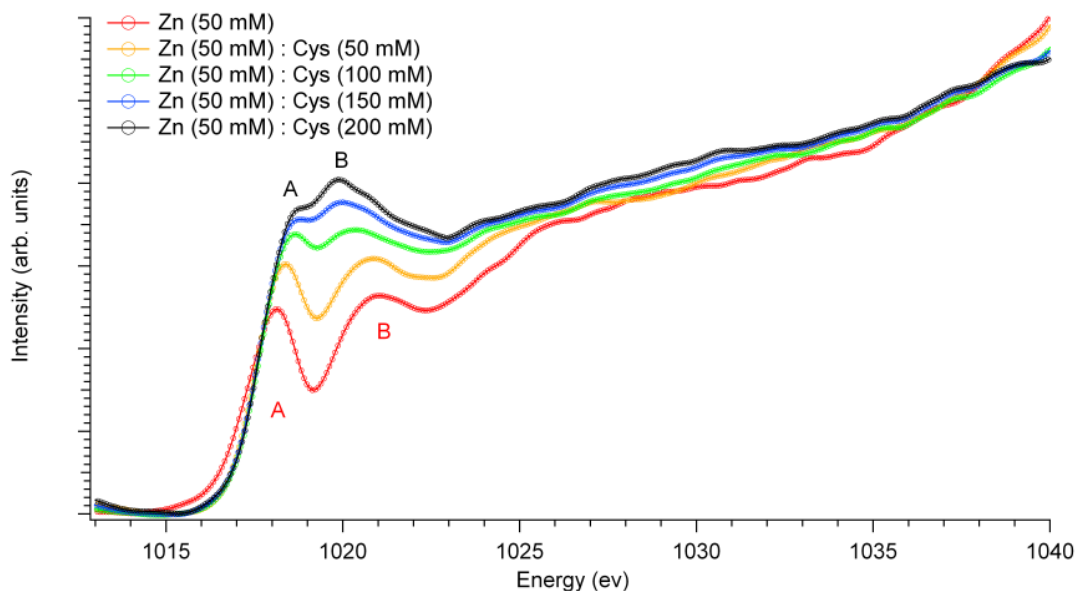

Figure 5.10: Zn^{2+} L-NEXAFS spectra for different concentration ratio of Zn:cysteine at pH 5
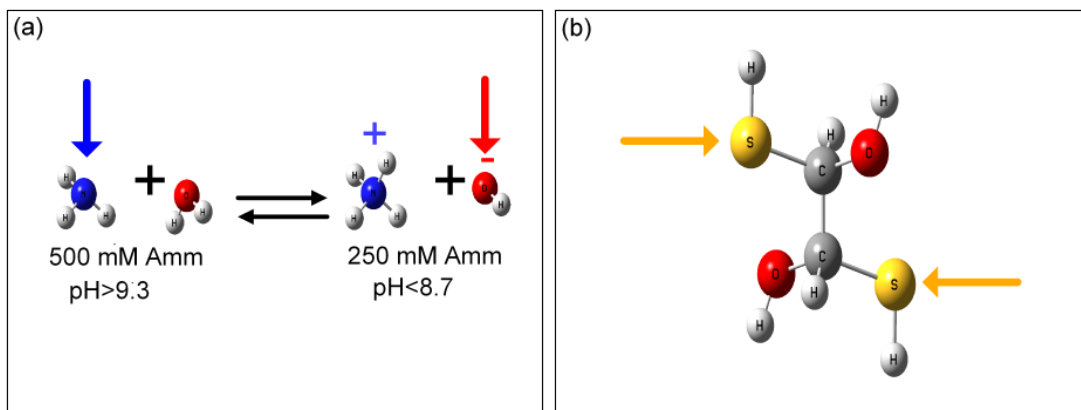
Figure 5.11: Chemical structure for dissolving (a) ammonia (Amm) in water, where at low concentration the hydroxyl group is the chelating one, while at high concentration, the NH_3 group is the chelating one (arrows), (b) dithiothreitol (DTT), where the arrows indicate the chelating groups.

In order to distinguish the effect of SH chelating group by Cys from the NH_2 group by Cys and His, two ligand model molecules have been investigated for complex formation with Zn^{2+}. These model molecules are dithiothreitol (DTT) and ammonia (Amm), the structures are shown in Fig.5.11. At low concentration ammonia acts as a base $(NH_4^+ + OH^-)$, while by adding extra ammonia NH_3 will form and act as a ligand $(NH_3 + H_2O)$, as it is known in coordination chemistry [141]. We assume that the effect of NH_3 group upon complex formation with Zn^{2+} will be similar to the amino group of the amino acids. The effect on the Zn^{2+} NEXAFS spectra introduced by adding ammonia is presented in Fig.5.12. Hydroxyl ions acting as a base at 250 mM in the solution causes peak A to shift to 1018.8 eV, while peak B shifts to 1021 eV. Upon increasing the amount of ammonia in the solution to 500 mM, NH_3 will form and act as ligand with Zn^{2+}. The effect of the NH_3 as a ligand, as shown in Fig.5.12 has a similar effect as adding His to the Zn^{2+}: peak A is not affected, while peak B shifts to 1019.5 eV. Therefor, we conclude that His is forming a complex with Zn^{2+} mainly via the NH_2 group. These results thus support the existence of the structure shown in Fig.5.7.c for the complex formation between His and Zn^{2+}, in accord with similar results from stability constant measurement [142]. On the other hand, this experiment provides no indication for the existence of other complexes, where the COO^- group is involved. In such a case, we would expect the behavior seen in the 250 mM ammonia with

Zn^{2+} spectra, where OH^-, which is electronically similar to COO^-, is involved in complex formation. Based on the earlier assignment for the origin of peak B, His is primarily affecting the Zn^{2+} s- states upon complex formation with Zn^{2+}.
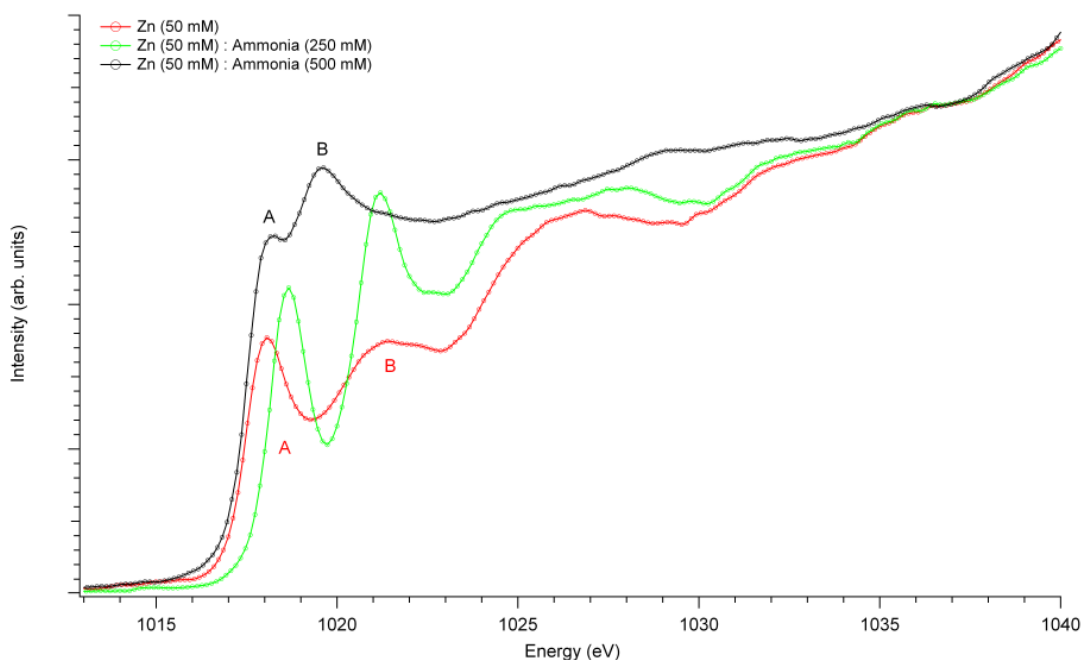

Figure 5.12: Zn^{2+} L-NEXAFS spectra for Zinc ion with ammonia where ammonia act as an base (green) and as a ligand (black).

In Cys, a different behavior is observed as seen in Fig.5.10. As we have speculated earlier that the SH group in Cys may cause the shift of peak A. To examine this, NEXAFS spectra for the L-edge of Zn^{2+} have been measured after adding DTT (the structure is shown in Fig.5.11.b) at different concentration. It is known that DTT is a strong chelating agent with two SH groups [152]. As shown in Fig.5.13, by complex formation between DTT and Zn^{2+}, peak A is shifted to 1018.8 eV and peak B is shifted to 1020 eV. Since the same behavior is observed for Cys, one can conclude that the SH group of Cys is the one which is forming a complex with Zn^{2+} at pH $\cong$ 5. Moreover, this group affects both zinc s- and d-states upon formation of a complex. Again, these results support one of the models which has been proposed by the stability constant measurement depicted in Fig.5.8.c [148, 153]. As in the case of His, no evidence for a complex formation via the COO^- is observed in this study, although this has been proposed in Refs. [148, 153]. Thus, the free Cys molecule chelate Zn^{2+}

in the same way as in the protein, although other functional groups (which are consumed in the peptide bond in case of the protein) would be available.
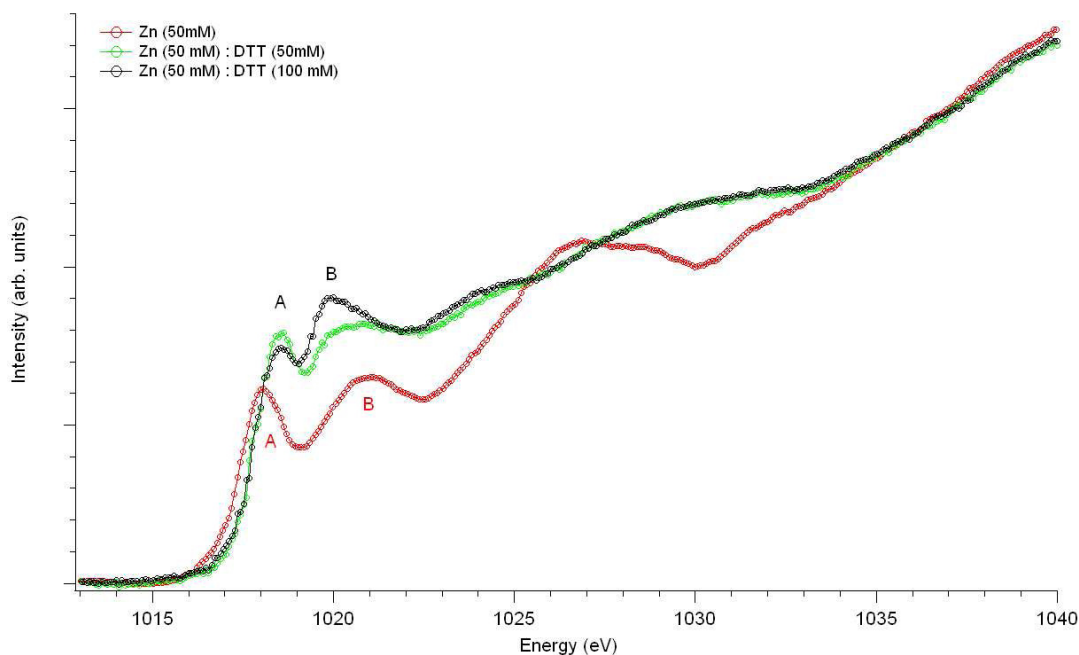

Figure 5.13: Zn^{2+} L-NEXAFS spectra for different concentration ratio of Zn:dithiothreitol (DTT).

Finally, we briefly investigate the effect of the Cl^- counter ion on the complex formation between the Zn^{2+} and the amino acids, since Zn^{2+} is obtained upon dissolving $ZnCl_2$ in water. The effect of this ligand on the L-edge of Zn^{2+} is investigated as shown in Fig.5.14 by measuring the concentration range from 10 mM up to 500 mM of $ZnCl_2$. No significant change in the L-edge spectra of the Zn^{2+} is observed over the concentration range from 10 mM to 100 mM. It has been shown before that at concentrations lower than 50 mM Ni^{2+} ions are fully hydrated and no ion-pairing exists in the solution [68], so our observation for Zn^{2+} is in line with the observation for Ni^{2+}. On the other hand, for 500 mM $ZnCl_2$, a significant shift of peak A to 1018.8 eV, and B to 1021.5 eV is observed, which can be attributed to the ion-pairing between the Zn^{2+} and Cl^-. This rigid band shift is about 1 eV in magnitude, similar to the shift observed upon adding 250 mM ammonia, where Zn^{2+} interacts with OH^-. As no peak shift is observed up to 100 mM, one can in the first approximation neglect the effect of the Cl^- ions in the complex for-

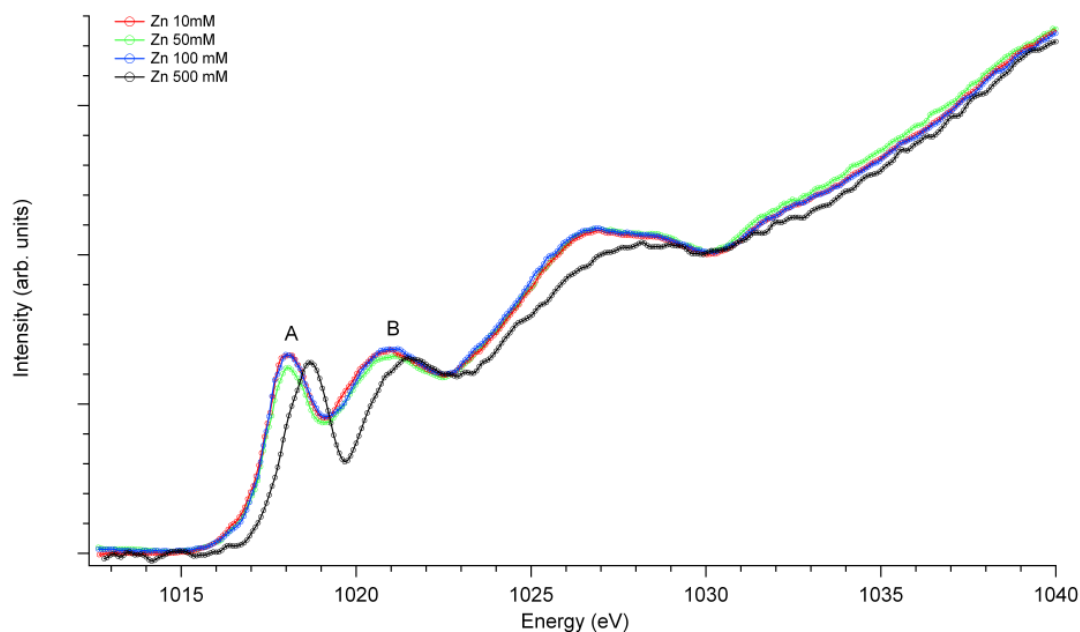mation between the Zn^{2+} and the amino acids at $ZnCl_2$ concentration of 50 mM.

Figure 5.14: Zn^{2+} L-NEXAFS spectra for different concentration of $ZnCl_2^{aq}$ solution

5.2.3 Conclusions

The effect of the cysteine (Cys), and the histidine (His) upon complex formation with Zn^{2+} is investigated by the means of NEXAFS at the L-edge of Zn^{2+}. Significantly different effects in the spectra are observed upon chelation with Hys and Cys. This different behavior is due to the SH group of the Cys, which is absent in His. The observed effects on the NEXAFS spectra are distinguished by comparing the effect of model ligands on the Zn^{2+} L absorption edge. NH_3 shows the same effect on the L-edge of Zn^{2+} as His; based on this observation, one can expected a chelation of His to Zn^{2+} via the amino group. On the other hand, adding dithiothreitol (DTT) to Zn^{2+}, the same change in the L-edge is observed as for Cys. Based on these observations, we expect a chelation of Cys to Zn^{2+} via the SH group, which is the same way of the chelation seen in zinc finger proteins.

More indirect evidence (the presence of OH^- when diluted ammonia is added)

suggests that the effect of the anionic carboxilic COO^- group can be in first approximation neglected for the chelation of Zn^{2+} for Cys and His. Cys affects the Zn s- states upon chelation of Zn^{2+}, while His affects both d- and s- states.